Phenomenological investigation of the beauty content of a proton in the framework of k_t-factorization using Kimber-Martin-Ryskin and Martin-Ryskin-Watt unintegrated parton distributions

N. Olanj[*]

*Department of Physics, Faculty of Science, Bu-Ali Sina University,
65178, Hamedan, Iran*

In this paper, we address the reduced beauty cross section [$\sigma_{\mathrm{red}}^{b\bar{b}}(x, Q^2)$] and the beauty structure function [$F_2^{b\bar{b}}(x, Q^2)$], to study the beauty content of a proton. We calculate $\sigma_{\mathrm{red}}^{b\bar{b}}$ and $F_2^{b\bar{b}}$ in the k_t-factorization formalism by using the integral form of the Kimber-Martin-Ryskin and Martin-Ryskin-Watt unintegrated parton distribution function (KMR and MRW-UPDF) with the angular ordering constraint (AOC) and the *MMHT*2014 *PDF* set as the input. Recently Guiot and van Hameren demonstrated that the upper limit, $k_{\max}$, of the transverse-momentum integration performed in the k_t-factorization formalism should be almost equal to Q, where Q is the hard scale, otherwise it leads to an overestimation of the proton structure function [$F_2(x, Q^2)$]. In the present work, we show that $k_{\max}$ cannot be equal to Q at low and moderate energy region, and also by considering the gluon and quark contributions to the same perturbative order and a physical gauge for the gluon, i.e., $A^\mu q'_\mu = 0$ in the calculation of $F_2^{b\bar{b}}$ in the k_t-factorization formalism, we do not encounter any overestimation of the theoretical predictions due to different choices of $k_{\max} > Q$. Finally, the resulted $\sigma_{\mathrm{red}}^{b\bar{b}}$ and $F_2^{b\bar{b}}$ are compared to the experimental data and the theoretical predictions. In general, the extracted $\sigma_{\mathrm{red}}^{b\bar{b}}$ and $F_2^{b\bar{b}}$ based on the KMR and MRW approaches are in perfect agreement with the experimental data and theoretical predictions at high energies, but at low and moderate energies, the one developed from the KMR approach has better consistency than that of the MRW approach.

DOI: 10.1103/PhysRevD.110.036009

I. INTRODUCTION

The study of the charm and beauty content of a proton in deep inelastic ep scattering at HERA plays an important role in the investigation of the theory of the perturbative quantum chromodynamics (pQCD) at the small Bjorken scale (x) [1–3], the electroweak Higgs boson production at the LHC [4] and hadron-hadron differential cross sections.

Recently, we investigated the charm content of a proton in the frameworks of the KMR [5] and MRW [6] approaches by calculating the charm structure function $F_2^{c\bar{c}}(x, Q^2)$ [7] in the k_t-factorization formalism [8–12]. We showed that the calculated charm structure functions by using the MRW-UPDF and KMR-UPDF are consistent with the experimental data and the theoretical predictions

based on the general-mass variable-flavor-number scheme (GMVFNS) [13], the LO collinear procedure and the saturation model introduced by Golec-Biernat and Wüsthoff [14]. Also, in the Ref. [15], the b-quark contribution to the inclusive proton structure function $F_2(x, Q^2)$ at high values of Q^2 has been investigated at the leading-order k_t-factorization approach using KMR-UPDF and only considering the gluon contribution. Recently, in the Ref. [16], measurements of charm and beauty production cross section in deep inelastic ep scattering at HERA from the H1 and ZEUS Collaborations are combined and results for the so-called reduced charm and beauty cross section [$\sigma_{\mathrm{red}}^{q\bar{q}}(x, Q^2), q = c, b$] are obtained in the kinematic range of negative four-momentum transfer squared ($-q^2 = Q^2$) of the photon 2.5 GeV$^2 \leq Q^2 \leq 2000$ GeV^2 and Bjorken scaling variable $3 \times 10^{-5} \leq x_{Bj} \leq 5 \times 10^{-2}$. The double-differential cross section for the production of a heavy flavor of type q ($q = c, b$) may then be written in terms of the heavy-flavor contributions of the structure functions $F_2(x, Q^2)$ [$F_T(x, Q^2) + F_L(x, Q^2)$] and $F_L(x, Q^2)$ [17,18], as follows:

$$\frac{d^2\sigma^{q\bar{q}}}{dxdQ^2} = \frac{4\pi\alpha^2(Q^2)}{Q^4}\left[\frac{1+(1-y)^2}{2x}F_T^{q\bar{q}}(x,Q^2) + \frac{1-y}{x}F_L^{q\bar{q}}(x,Q^2)\right]$$

$$= \frac{2\pi\alpha^2(Q^2)}{xQ^4}\left[(1+(1-y)^2)F_2^{q\bar{q}}(x,Q^2) - y^2F_L^{q\bar{q}}(x,Q^2)\right], \qquad (1)$$

where $y = \frac{Q^2}{xs}$ (s is *CM* energy squared) denotes the lepton inelasticity, the fraction of energy transferred from the electron in the fixed proton frame. The reduced cross sections are defined, as follows:

$$\sigma_{\text{red}}^{q\bar{q}}(x,Q^2) = \frac{d^2\sigma^{q\bar{q}}}{dxdQ^2} \cdot \frac{xQ^4}{2\pi\alpha^2(Q^2)(1+(1-y)^2)}$$

$$= F_2^{q\bar{q}}(x,Q^2) - \frac{y^2}{1+(1-y)^2}F_L^{q\bar{q}}(x,Q^2). \qquad (2)$$

In expressing the importance of the investigation of the proton beauty contents in this paper, it should be noted that the reduced cross section [$\sigma_{\text{red}}^{q\bar{q}}(x,Q^2)$] is dependent on the heavy-flavor longitudinal structure function [$F_L^{q\bar{q}}(x,Q^2)$]. Therefore, since the longitudinal structure function is directly sensitive to the gluon distributions, the calculations of the reduced cross section are beyond the standard collinear factorization procedure, i.e., the k_t-factorization formalism.

In this work, we use the integral form of MRW-UPDF and KMR-UPDF with the angular ordering constraint (AOC) [19] and the ordinary parton distribution functions (the cutoff independent PDF) according to the investigations carried out in the Refs. [19,20] as input in the k_t-factorization formalism to calculate the reduced cross section of production of a beauty quark pair in the final state of the deep inelastic ep scattering, [$\sigma_{\text{red}}^{b\bar{b}}(x,Q^2)$] and the beauty structure function [$F_2^{b\bar{b}}(x,Q^2)$]. It is worth mentioning that in the Refs. [19,20], it is stated that "the differential version of KMR prescription and the implementations of angular (strong) ordering constraints [AOC (SOC)], cause the negative-discontinuous UPDF with the ordinary parton distribution functions as the input and finally leads to results far from experimental data, but those the proton (longitudinal) structure functions calculated based on the integral prescription of the KMR-UPDF with the AOC and the ordinary PDF as the input are reasonably consistent with the experimental data." Then the predictions of these two approaches by using the *MMHT*2014-*LO* and *MMHT*2014-*NLO* set of the PDF [21] as input for the reduced beauty cross section are compared to the combined data of the H1 and ZEUS Collaborations at *HERA* [16] and theoretical predictions based on the *HERAPDF*2.0 *FF*3A set [22]. Also, the resulted beauty structure function is compared to the predictions of the *MSTW*08 − *NLO QCD* fits [23] and

the ZEUS measurements [2,24,25]. As shown in Refs. [26,27], UPDF with different input PDF sets are almost very similar and stable, so we can still use *MMHT*2014 PDF set instead of the new *MSHT*20 PDF set [28] in this work. In general, it is shown that the calculated reduced beauty cross section ($\sigma_{\text{red}}^{b\bar{b}}$) and the beauty structure function ($F^{b\bar{b}}$) based on the UPDF of the two approaches are very consistent with the experimental data, especially at high energies. However, the reduced beauty cross sections and the beauty structure functions, which are extracted from the KMR approach, have a better agreement with the experimental data with respect to that of MRW at low and moderate energies.

It should be noted that the k_t-factorization formalism is computationally more straightforward than the theory of the $pQCD$. The discrepancy between the $pQCD$ and the k_t-factorization prediction can be reduced by refitting the input integrated PDF [29] and using the cutoff dependent PDF [30]. As explained in the Ref. [29], this treatment is adequate for initial investigations and descriptions of exclusive processes.

It is worth mentioning that recently Guiot and van Hameren (*GvH*) encountered an overestimation of the exact structure function by calculate the proton structure function [$F_2(x,Q^2)$] in the k_t-factorization formalism at order $O(\lambda^2)$, with λ the coupling of the Yukawa theory by using the differential form of the KMRW-UPDF computed in the Yukawa theory only considering the quark contributions [31]. Therefore, GvH argued that the upper limit, $k_{\max}$, of the transverse-momentum integration performed in the k_t-factorization formalism is equal to $\mu_F \sim Q$ (Q is the hard scale) used to factorize the cross section into an off-shell hard coefficient and a universal factor. In the present work, we show that $k_{\max}$ cannot be equal to Q at low and moderate energy region (2.5 GeV$^2 \leq Q^2 \leq 120$ GeV^2), and also by considering the gluon and quark contributions to the same perturbative order and a physical gauge for the gluon, i.e., $A^\mu q'_\mu = 0$ in the calculation of $F_2^{b\bar{b}}(x,Q^2)$ and $F_L^{b\bar{b}}(x,Q^2)$ in the k_t-factorization formalism, we do not encounter any overestimation of the theoretical predictions due to different choices of $k_{\max} > Q$.

Due to the importance of this subject, in our previous articles, we investigated the general behavior and stability of the KMR and MRW approaches [26,32–39] and in this paper, we study the beauty content of a proton by examining the reduced cross section [$\sigma_{\text{red}}^{b\bar{b}}(x,Q^2)$] and the beauty structure function [$F^{b\bar{b}}(x,Q^2)$]. Also, we have

successfully used KMR-UPDF in our previous articles, to calculate the inclusive production of the W and Z gauge vector bosons [40,41], the semi-NLO production of $Higgs$ bosons [42], the production of forward-center and forward-forward dijets [43], the prompt-photon pair production [44], the single-photon production [45] and the charm structure function [7]. We explored the phenomenology of the integral and the differential versions of the KMR-UPDF using the angular (strong) ordering [AOC (SOC)] constraints in the Ref. [19]. Also, among the applications of these UPDF, one can refer to the Refs. [46–49].

So, the paper is organized as follows: an overview of the KMR and MRW approaches to generating UPDF and calculation of the beauty contribution to the proton structure function [$F_2^{b\bar{b}}(x, Q^2)$] and the proton longitudinal structure function [$F_L^{b\bar{b}}(x, Q^2)$] based on the k_t-factorization formalism are provided in Sec. II. Finally, the results of the reduced beauty cross section and the beauty structure function in the k_t-factorization formalism using the KMR-UPDF and MRW-UPDF as input are presented in section *III*.

II. KMR-UPDF, MRW-UPDF APPROACHES AND $F_2^{b\bar{b}}(x,Q^2)$ AND $F_L^{b\bar{b}}(x,Q^2)$ IN THE k_t-FACTORIZATION FORMALISM

A brief review of the KMR [5] and MRW [6] approaches to generating UPDF [$f_a(x, k_t^2, \mu^2)$ at the LO and NLO levels, respectively, where x, k_t, and μ are the longitudinal momentum fraction, the transverse momentum, and the factorization scale, respectively] is provided in this section. The KMR and MRW formalisms are based on the DGLAP equations using some modifications due to the separation of the virtual and real parts of the evolutions.

The KMR approach leads to the following integral forms for the quark and gluon UPDF at the LO level, respectively

$$f_q(x, k_t^2, \mu^2) = T_q(k_t, \mu)\frac{\alpha_s(k_t^2)}{2\pi}$$
$$\times \int_x^{1-\Delta} dz \left[P_{qq}(z)\frac{x}{z}q\left(\frac{x}{z}, k_t^2\right) \right.$$
$$\left. + P_{qg}(z)\frac{x}{z}g\left(\frac{x}{z}, k_t^2\right) \right], \quad (3)$$

$$f_g(x, k_t^2, \mu^2) = T_g(k_t, \mu)\frac{\alpha_s(k_t^2)}{2\pi}$$
$$\times \int_x^{1-\Delta} dz \left[\sum_q P_{gq}(z)\frac{x}{z}q\left(\frac{x}{z}, k_t^2\right) \right.$$
$$\left. + P_{gg}(z)\frac{x}{z}g\left(\frac{x}{z}, k_t^2\right) \right], \quad (4)$$

where $P_{aa'}(x)$ are the corresponding splitting functions and the survival probability factors, T_a, is evaluated from

$$T_a(k_t, \mu) = \exp\left[-\int_{k_t^2}^{\mu^2} \frac{\alpha_s(k_t'^2)}{2\pi}\frac{dk_t'^2}{k_t'^2} \right.$$
$$\left. \times \sum_{a'} \int_0^{1-\Delta} dz' P_{a'a}(z') \right], \quad (5)$$

where Δ is a cutoff to prevent the integrals from becoming singular at $z = 1$ (arises from the soft gluon emission). By considering the angular ordering constraint (AOC), which is the consequence of the coherent gluon emissions, the cutoff is equal to $\frac{k_t}{\mu+k_t}$ and UPDF extend smoothly into the domain $k_t > \mu$. It should be mentioned that in this approach, T_a is considered to be unity for $k_t > \mu$. Therefore $k_{\max} = \mu \sim Q$ is not an intrinsic property of the unintegrated parton distribution function.

The MRW approach leads to the following integral forms for the quark and gluon UPDF at the NLO level

$$f_a(x, k_t^2, \mu^2) = \int_x^1 dz T_a(k^2, \mu^2)\frac{\alpha_s(k^2)}{2\pi}$$
$$\times \sum_{b=q,g} P_{ab}^{(0+1)}(z)b\left(\frac{x}{z}, k^2\right)\Theta(\mu^2 - k^2), \quad (6)$$

where

$$P_{ab}^{(0+1)}(z) = P_{ab}^{(0)}(z) + \frac{\alpha_s}{2\pi}P_{ab}^{(1)}(z),$$
$$k^2 = \frac{k_t^2}{1-z}, \quad (7)$$

and

$$T_a(k^2, \mu^2) = \exp\left(-\int_{k^2}^{\mu^2} \frac{\alpha_s(\kappa^2)}{2\pi}\frac{d\kappa^2}{\kappa^2} \right.$$
$$\left. \times \sum_{b=q,g} \int_0^1 d\zeta \zeta P_{ba}^{(0+1)}(\zeta) \right). \quad (8)$$

$P_{ab}^{(0)}$ and $P_{ab}^{(1)}$ functions in the above equations correspond to the LO and NLO contributions of the splitting functions, respectively, which are given in the Ref. [50]. In the MRW approach, unlike the KMR approach, the cutoff is imposed only on the terms in which the splitting functions are singular, i.e., the terms that include P_{qq} and P_{gg}, also, the scale $k^2 = \frac{k_t^2}{1-z}$ is used instead of the scale k_t^2. For more details see Ref. [35].

In the following, we briefly present the formulations of the beauty structure function [$F_2^{b\bar{b}}(x, Q^2)$] and the beauty longitudinal structure function [$F_L^{b\bar{b}}(x, Q^2)$] in the
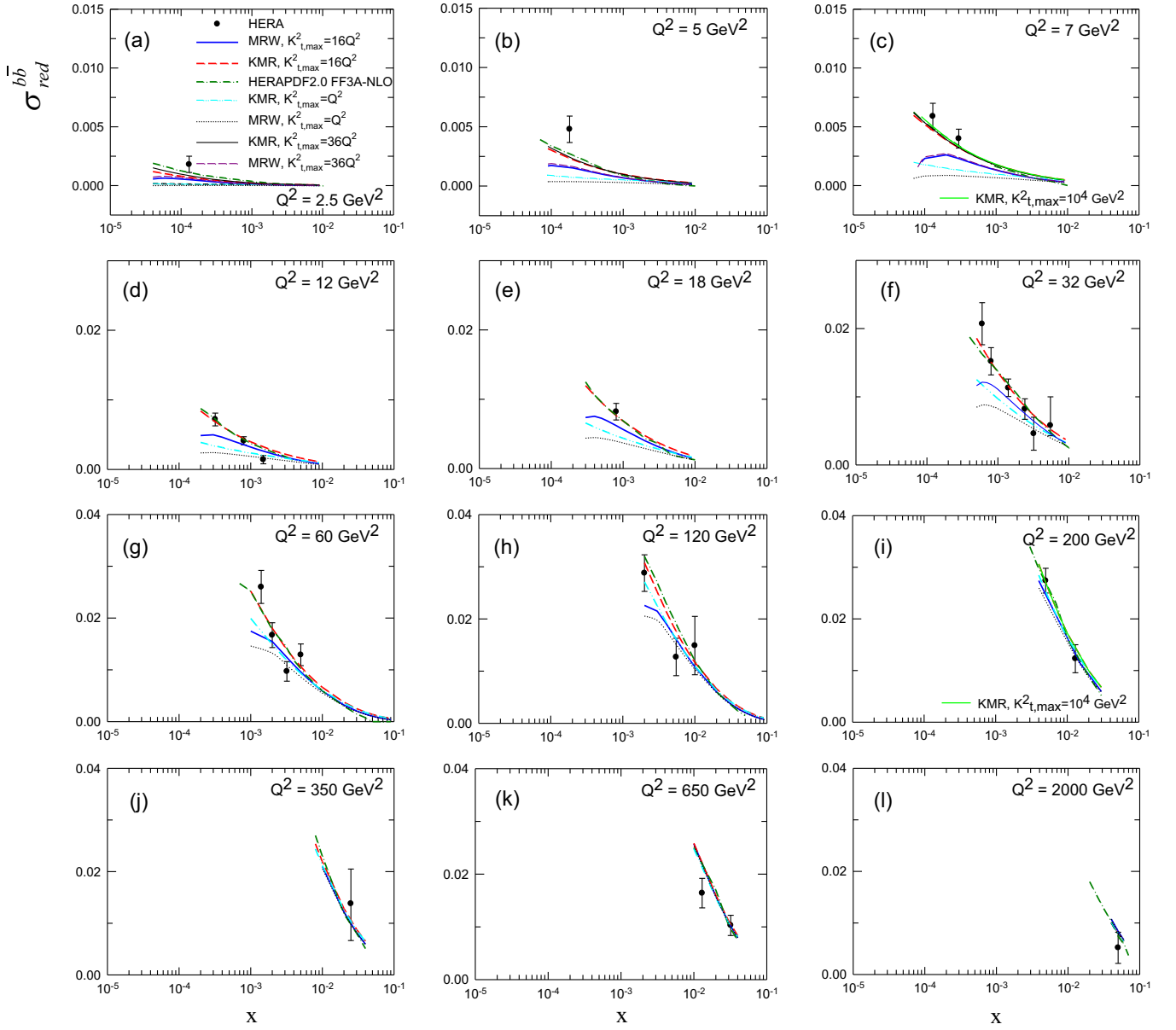
FIG. 1.   The reduced beauty cross section as a function of x for various Q^2 values in panels (a)–(l). See the text for more explanations about the different panels.

k_t-factorization formalism. By considering the gluon and quark contributions to the same perturbative order and a physical gauge for the gluon, i.e., $A^\mu q'_\mu = 0$ $(q' = q + xp)$, the beauty structure function $F_2^{b\bar{b}}(x, Q^2)$ is given by the sum of the gluon contribution [the subprocess $g \to q\bar{q}$, the Eq. (9)] and the quark contribution [the subprocess $q \to qg$, the Eq. (13)] according to the Eqs. (8) and (12) of the Ref. [7]. For the gluon contribution

$$F_{2\,g \to q\bar{q}}^{b\bar{b}}(x, Q^2) = e_b^2 \frac{Q^2}{4\pi} \int_{k_0^2}^{k_{\max}^2} \frac{dk_t^2}{k_t^4} \int_0^1 d\beta \int_{k_0^2}^{k_{\max}^2} d^2\kappa_t \alpha_s(\mu^2) f_g\left(\frac{x}{z}, k_t^2, \mu^2\right) \Theta\left(1 - \frac{x}{z}\right)$$

$$\times \left\{ [\beta^2 + (1 - \beta^2)] \left(\frac{\kappa_t}{D_1} - \frac{(\kappa_t - k_t)}{D_2}\right)^2 + [m_b^2 + 4Q^2\beta^2(1 - \beta)^2] \left(\frac{1}{D_1} - \frac{1}{D_2}\right)^2 \right\}, \quad (9)$$

where

$$D_1 = \kappa_t^2 + \beta(1-\beta)Q^2 + m_b^2,$$
$$D_2 = (\boldsymbol{\kappa_t} - \boldsymbol{k_t})^2 + \beta(1-\beta)Q^2 + m_b^2, \qquad (10)$$

and

$$\frac{1}{z} = 1 + \frac{\kappa_t^2 + m_b^2}{(1-\beta)Q^2} + \frac{k_t^2 + \kappa_t^2 - 2\boldsymbol{\kappa_t} \cdot \boldsymbol{k_t} + m_b^2}{\beta Q^2}, \qquad (11)$$

where in the above equations, the variable β is defined as the light-cone fraction of the photon momentum carried by the internal quark and k_0 is chosen to be about 1 GeV. The graphical representations of k_t and κ_t are introduced in the Fig. 7 of the Ref. [35]. The scale μ controls both the unintegrated partons and the QCD coupling constant (α_s) and it is chosen as follows:

$$\mu^2 = k_t^2 + \kappa_t^2 + m_b^2. \qquad (12)$$

It should be mentioned that the imposition of angular ordering constraint (AOC) at the last step of the evolution instead of the strong ordering constraint (SOC) leads to physically reasonable unintegrated parton distribution functions which extend smoothly into the domain $k_t > \mu$ [5]. Therefore, the acceptable value of $k_{\max}$ is the value that does not change the result of structure function by increasing it. For example, in Ref. [17], $k_{\max}$ is considered equal to $4Q$.

For the quark contribution

$$F_{2q \to qg}^{b\bar{b}}(x, Q^2) = e_b^2 \int_{k_0^2}^{Q^2} \frac{d\kappa_t^2}{\kappa_t^2} \frac{\alpha_s(\kappa_t^2)}{2\pi} \int_{k_0^2}^{\kappa_t^2} \frac{dk_t^2}{k_t^2} \int_x^{\frac{Q}{(Q+k_t)}} dz$$
$$\times \left[f_b\left(\frac{x}{z}, k_t^2, Q^2\right) + f_{\bar{b}}\left(\frac{x}{z}, k_t^2, Q^2\right) \right]$$
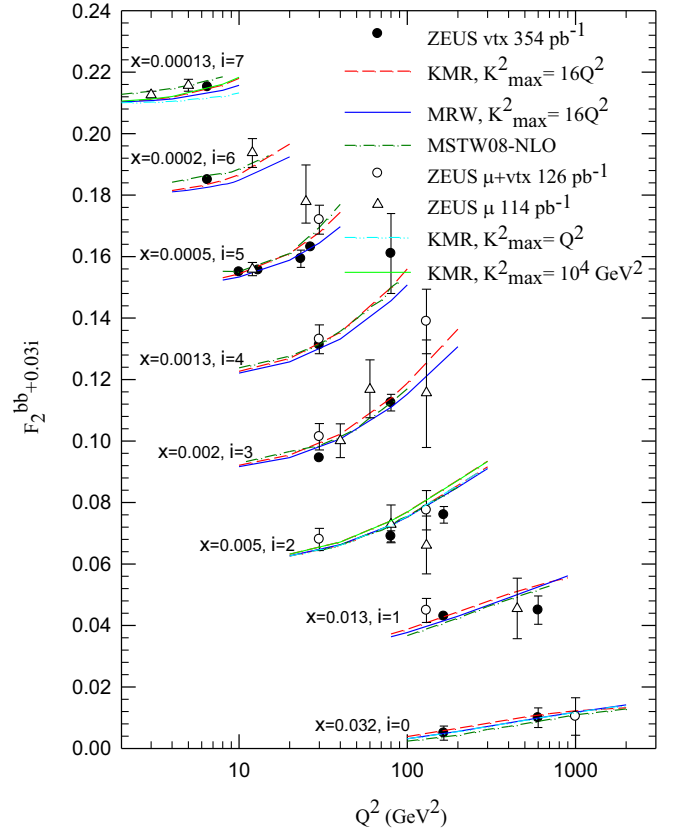$$\times P_{qq}(z). \qquad (13)$$

FIG. 2. The beauty structure function as a function of Q^2 for various x values. See the text for more explanations.

In this paper, the mass of beauty quark is considered to be $m_b = 4.18$ GeV. See Ref. [7] for more details.

As mentioned in Ref. [7], the dominant mechanism of the proton c, b-quark electroproduction is the subprocess $g \to q\bar{q}$, and since we are working in the small x region (i.e., the high energy region), we ignored the contribution of the nonperturbative region. According to the above, the beauty longitudinal structure function [$F_L^{b\bar{b}}(x, Q^2)$] in the k_t-factorization approach is presented as follows:

$$F_L^{b\bar{b}}(x, Q^2) = \frac{Q^4}{\pi^2} e_b^2 \int_{k_0^2}^{k_{\max}^2} \frac{dk_t^2}{k_t^4} \Theta(k^2 - k_0^2) \int_0^1 d\beta \int_{k_0^2}^{k_{\max}^2} d^2\kappa_t \alpha_s(\mu^2)\beta^2(1-\beta)^2 \left(\frac{1}{D_1} - \frac{1}{D_2}\right)^2$$
$$\times f_g\left(\frac{x}{z}, k_t^2, \mu^2\right) + e_b^2 \frac{\alpha_s(Q^2)}{\pi} \frac{4}{3} \int_x^1 \frac{dy}{y} \left(\frac{x}{y}\right)^2 [q(y, Q^2) + \bar{q}(y, Q^2)], \qquad (14)$$

where $y = x(1 + \frac{\kappa_t'^2 + m_b^2}{\beta(1-\beta)Q^2})$ [in which $\boldsymbol{\kappa_t'} = \boldsymbol{\kappa_t} - (\mathbf{1} - \boldsymbol{\beta})\mathbf{k_t}$] and the variables of the above equation are the same as the variables of the beauty structure function [$F_2^{b\bar{b}}(x, Q^2)$]. It should be noted that the first term is derived with the use of a pure gluon contribution from the perturbative region in the k_t-factorization approach. The second term is the beauty

quark contribution in the longitudinal structure function which comes from the collinear factorization.

III. RESULTS, DISCUSSIONS, AND CONCLUSIONS

As mentioned before, the purpose of this work is a detailed investigation of the beauty content of a proton in
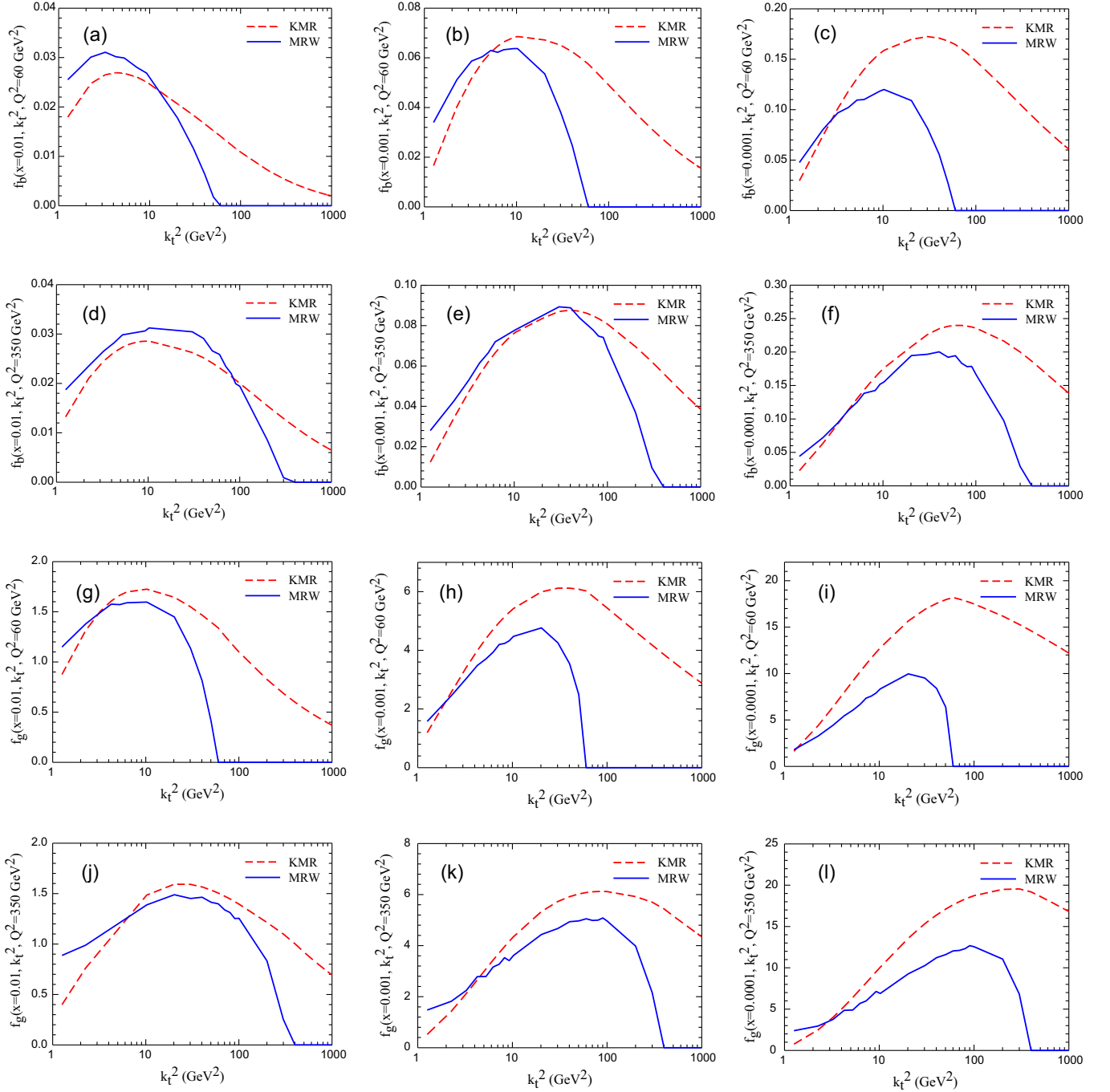
FIG. 3. The unintegrated beauty quark [panels (a)–(f)] and gluon [panels (g)–(l)] distribution functions versus $k_t{}^2$ with the KMR (MRW) prescription by using the $MMHT2014 - LO$ ($MMHT2014 - NLO$) as the inputs.

the framework of k_t-factorization using KMR and MRW approaches to generate the UPDF, validate these two approaches and also investigation the upper limit of transverse momentum (k_{max}) in the k_t-factorization formalism. For this purpose, the reduced beauty cross sections [$\sigma_{red}^{b\bar{b}}(x, Q^2)$, the Eq. (2)] are calculated by using the beauty structure functions [$F_2^{b\bar{b}}(x, Q^2)$, the sum of the Eqs. (9) and (13)] and the beauty longitudinal structure functions

[$F_L^{b\bar{b}}(x, Q^2)$, the Eq. (14)] in the k_t-factorization formalism. The integral form of KMR-UPDF and MRW-UPDF, i.e., the Eqs. (3), (4), and (6) with the AOC are used as input of the beauty structure functions and the beauty longitudinal structure functions in the k_t-factorization formalism with different $k_{max} \geq Q$.

In the Fig. 1, the reduced beauty cross section ($\sigma_{red}^{b\bar{b}}$) are displayed in the framework of k_t-factorization using the

KMR and MRW approaches as a function of x for different values of $Q^2 = 2.5, 5, 7, 12, 18, 32, 60, 120, 200, 350, 650$, and $2000 \times GeV^2$ with the input $MMHT2014$ set of PDF (to generate the UPDF) at the LO and NLO approximations, respectively, with $k_{max}^2 = Q^2, 16Q^2$ in all panels, $k_{max}^2 = 36Q^2$ in panels (a)–(c) and $k_{max}^2 = 10^4 GeV^2$ in panels (c) and (i). These results are compared to the combined data of the $H1$ and ZEUS Collaborations at HERA [16] (the full circle points) and theoretical predictions based on the $HERAPDF2.0$ $FF3A$ set [22] (dash-dot curves). In the Fig. 2, the obtained results from the calculations of the beauty structure functions are presented as a function of Q^2 for various x values using the KMR ($MMHT2014 - LO$ PDF, dash curves) and MRW ($MMHT2014 - NLO$ PDF, full curves) approaches with $k_{max}^2 = Q^2$ (at $i = 0$, 2 and 7), $16Q^2$ (at all i) and 10^4 GeV^2 (at $i = 2$ and 7). These results are compared to the experimental measurements of ZEUS (filled circles [2], open circles [24] and open triangles [25]) and the predictions of $MSTW08 - NLO$ QCD calculations [23]. To provide a clear comparison between the frameworks of the KMR and MRW approaches, we have plotted the KMR-UPDF (dash curves) and MRW-UPDF (full curves) versus k_t^2 at typical values of $x = 0.01, 0.001$, and 0.0001 and the factorization scales $Q^2 = 60$ and 350 GeV^2 for the beauty and gluon partons, in the Fig. 3. Also, the beauty and gluon PDF at scales $Q^2 = 60$ and 350 GeV^2 are plotted by using the $MMHT2014$-LO (dash curves) and $MMHT2014$-NLO (full curves) [21] in Fig. 4. It should be mentioned that in the calculations related to the

Figs. 1–3, we consider the QCD coupling constant, $\alpha_s(M_z^2)$, to be the same as those used in fitting the input PDF to the KMR-UPDF and MRW-UPDF, i.e., $\alpha_{s,LO}(M_z^2) = 0.135$ and $\alpha_{s,NLO}(M_z^2) = 0.118$, respectively.

In general, the extracted $\sigma_{red}^{q\bar{q}}$ and $F_2^{b\bar{b}}(x, Q^2)$ based on both the KMR and MRW approaches are in perfect consistent with the experimental data [16,23] and the theoretical predictions [2,22,24,25] at high energies, but the one developed from the KMR approach has a better agreement with the experimental data and the theoretical predictions with respect to that of MRW approach at low and moderate energies.

As shown in the Figs. 1 and 2, and we expected according to the Figs. 3 and 4 [see panels (d) and (j) of the Fig. 3 (the large x and high energy region) and the Fig. 4], the results of the KMR and MRW approaches are very close to each other at the high hard scale (Q^2) and large x, but they become separated as the hard scale and x decrease. It should be noted that this decrease in difference with increasing hard scale Q and x is due to the use of the scale $k^2 = \frac{k_t^2}{1-z}$, the coupling constant $\alpha_{s,NLO}(M_z^2) = 0.118$ and $MMHT2014$-NLO PDF set instead of the scale k_t^2, the coupling constant $\alpha_{s,LO}(M_z^2) = 0.135$ and $MMHT2014$-LO PDF set in the MRW approach. Note that this decrease cannot be a result of different use of cutoff and splitting functions.

It is clear in the Figs. 1 and 2 that at low and moderate x and low energy region (see the first 8 panels of the Fig. 1, $Q^2 \leq 120$ GeV^2 and $i = 7$ in the Fig. 2), there is no good agreement between the experimental data and the obtained
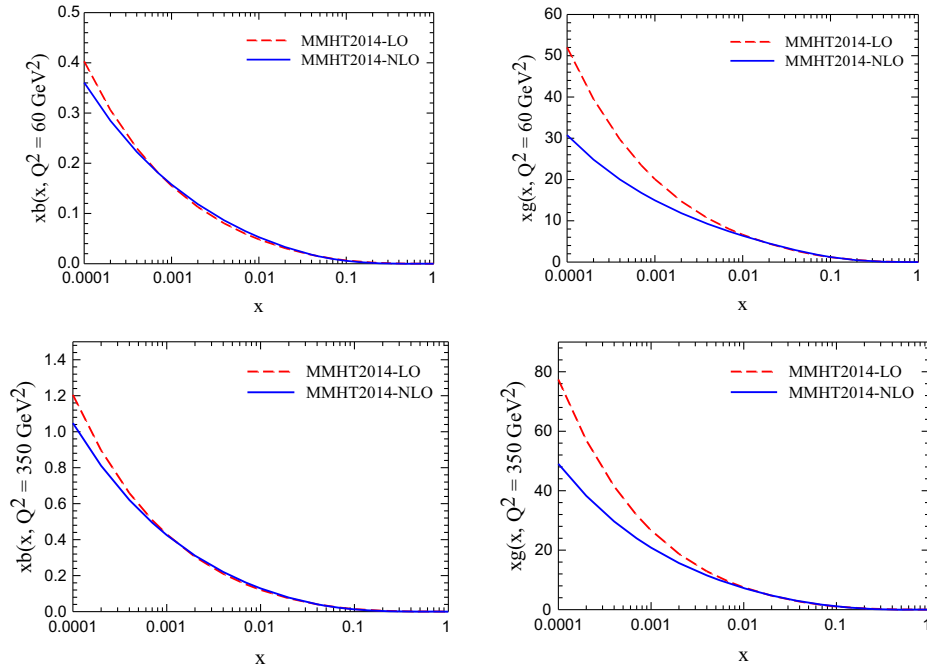

FIG. 4. The integrated beauty quark and gluon distribution functions at scale $Q^2 = 60$ and 350 GeV^2, by using the $MMHT2014 - LO$ (dash curves) and $MMHT2014 - NLO$ (full curves) [21].

results considering $k_{\max}^2 = Q^2$ and this is due to the non-negligibility value of KMR-UPDF in the $k_t > Q$ region at low x and Q^2 [see panels (c) and (i) of the Fig. 3]. But the results obtained from both KMR and MRW approaches, considering $K_{\max}^2 \geq 16Q^2$, have a good agreement with the theoretical predictions in all panels of the Figs. 1 and 2 (as mentioned in Ref. [17]). Also, at large x and high energy region (see the last 4 panels of the Fig. 1, $Q^2 \geq 200 GeV^2$ and $i = 2$ in the Fig. 2), with the increase of $k_{\max}^2$ from Q^2 to 10^4, the results are almost the same and this is due to the negligible value of KMR-UPDF and MRW-UPDF in the $k_t > Q$ region at large x and high values of Q^2 [see panels (d) and (j) of the Fig. 3]. It should be noted that according to the Figs. 1 and 2, we do not encounter any overestimation of the theoretical predictions with increasing $k_{\max}$.

Also, as it is clear in the Figs. 1 and 2, at high (low) energy region, the result of the reduced beauty cross section and the beauty structure functions calculations have not changed by increasing $k_{\max}$ from Q to $10Q$ (from $4Q$ to $10Q$), so $k_{\max} = Q$ ($k_{\max} = 4Q$) can be considered to save calculation time at high (low) energy.

It should be mentioned that the k_t-factorization is more computationally simpler than pQCD and is adequate for initial investigations and descriptions of exclusive processes [29]. The results of this paper are another confirmation of this matter. As it has been explained in the Ref. [29], we expect to reduce the discrepancy between the data and the k_t-factorization prediction by refitting the input integrated PDF and using the cutoff dependent PDF [30] as the input for the UPDF.

In conclusion, the extracted $\sigma_{\rm red}^{b\bar{b}}(x, Q^2)$ and $F_2^{b\bar{b}}(x, Q^2)$ in the k_t-factorization formalism by using the KMR-UPDF and MRW-UPDF are in a good agreement with the predictions of the pQCD and the experimental data, but those that are extracted from the KMR approach, have a perfect agreement with the experimental data. This issue cannot be unrelated to the consideration of $T_a = 1$ for $k_t > \mu$, which leads to the contribution of a NLO effect in the calculation of KMR-UPDF [5]. Also, according to the study conducted on the upper limit, $k_{\max}$, of the transverse-momentum integration performed in the k_t-factorization formalism, we hope that the computation time of the cross section at high energy region will be reduced by considering $k_{\max} = Q$.

ACKNOWLEDGMENTS

[1] G. Pancheri and Y. N. Srivastava, Introduction to the physics of the total cross section at LHC, Eur. Phys. J. C **77,** 150 (2017).

[2] H. Abramowicz *et al.* (ZEUS Collaboration), Measurement of beauty and charm production in deep inelastic scattering at HERA and measurement of the beauty-quark mass, J. High Energy Phys. 09 (2014) 127.

[3] R. Gauld, U. Haisch, B. D. Pecjak, and E. Re, Beauty-quark and charm-quark pair production asymmetries at LHCb, Phys. Rev. D **92,** 034007 (2015).

[4] F. Maltoni, Z. Sullivan, and S. Willenbrock, Higgs-boson production via bottom-quark fusion, Phys. Rev. D **67,** 093005 (2003).

[5] M. A. Kimber, A. D. Martin, and M. G. Ryskin, Unintegrated parton distributions, Phys. Rev. D **63,** 114027 (2001).

[6] A. D. Martin, M. G. Ryskin, and G. Watt, NLO prescription for unintegrated parton distributions, Eur. Phys. J. C **66,** 163 (2010).

[7] N. Olanj and M. Modarres, A detailed study of charm content of a proton in the frameworks of the Kimber-Martin-Ryskin and Martin-Ryskin-Watt approaches, Nucl. Phys. **A998,** 121735 (2020).

[8] S. Catani, M. Ciafaloni, and F. Hautmann, Gluon contributions to small χ heavy flavour production, Phys. Lett. B **242,** 97 (1990).

[9] S. Catani, M. Ciafaloni, and F. Hautmann, High energy factorization and small-x heavy flavour production, Nucl. Phys. **B366,** 135 (1991).

[10] J. C. Collins and R. K. Ellis, Heavy-quark production in very high energy hadron collisions, Nucl. Phys. **B360,** 3 (1991).

[11] S. Catani and F. Hautmann, High-energy factorization and small-x deep inelastic scattering beyond leading order, Nucl. Phys. **B427,** 475 (1994).

[12] M. Ciafaloni, $k_\perp$ factorization vs. renormalization group: A small-x consistency argument, Phys. Lett. **356,** 74 (1995).

[13] HERA combined results, HERAPDF table, https://www.desy.de/h1zeus/combined_results/herapdftable.

[14] L. Motyka and N. Timneanu, Unintegrated gluon in the photon and heavy quark production, Eur. Phys. J. C **27,** 73 (2003).

[15] A. V. Lipatov and N. P. Zotov, Deep inelastic beauty production at HERA in the k_T-factorization approach, J. High Energy Phys. 08 (2006) 043.

[16] H. Abramowicz *et al.* (H1 and ZEUS Collaborations), Combination and QCD analysis of charm and beauty production cross-section measurements in deep inelastic ep scattering at HERA, Eur. Phys. J. C **78,** 473 (2018).

[17] M. A. Kimber, Unintegrated parton distributions, Ph.D. thesis, University of Durham, 2001.

[18] R. K. Ellis, W. J. Stirling, and B. R. Webber, *QCD and Collider Physics* (Cambridge University Press, Cambridge, England, 1996).

[19] N. Olanj and M. Modarres, A phenomenological investigation of the integral and the differential versions of the Kimber–Martin–Ryskin unintegrated parton distribution functions using two different constraints and the MMHT2014 PDF, Eur. Phys. J. C **79,** 615 (2019).

[20] K. Golec-Biernat and A. M. Stasto, On the use of the KMR unintegrated parton distribution functions, Phys. Lett. B **781,** 633 (2018).

[21] L. A. Harland-Lang, A. D. Martin, P. Motylinski, and R. S. Thorne, Parton distributions in the LHC era: MMHT 2014 PDFs, Eur. Phys. J. C **75,** 204 (2015).

[22] H. Abramowicz *et al.* (H1 and ZEUS Collaborations), Combination of measurements of inclusive deep inelastic $e^{\pm}p$ scattering cross sections and QCD analysis of HERA data, Eur. Phys. J. C **75,** 580 (2015).

[23] A. D. Martin, W. J. Stirling, R. S. Thorne, and G. Watt, Parton distributions for the LHC, Eur. Phys. J. C **63,** 189 (2009).

[24] S. Chekanov *et al.* (ZEUS Collaboration), Measurement of charm and beauty production in deep inelastic ep scattering from decays into muons at HERA, Eur. Phys. J. C **65,** 65 (2010).

[25] H. Abramowicz *et al.* (ZEUS Collaboration), Measurement of beauty production in DIS and $F_2^{b\bar{b}}$ extraction at ZEUS, Eur. Phys. J. C **69,** 347 (2010).

[26] M. Modarres and H. Hosseinkhani, The new investigation of Kimber–Martin–Ryskin unintegrated partons, Few-Body Syst. **47,** 237 (2010).

[27] Z. Badieian Baghsiyahi, M. Modarresa, and R. Kord Valeshabadi, On validity of different PDFs sets using the proton k_t-factorization structure functions and the Gaussian k_t-dependence of KMR UPDFs, Eur. Phys. J. C **82,** 392 (2022).

[28] S. Bailey, T. Cridge, L. A. Harland-Lang, A. D. Martin, and R. S. Thorne, Parton distributions from LHC, HERA, Tevatron and fixed target data: MSHT20 PDFs, Eur. Phys. J. C **81,** 341 (2021).

[29] G. Watt, A. D. Martin, and M. G. Ryskin, Unintegrated parton distributions and electroweak boson production at hadron colliders, Phys. Rev. D **70,** 014012 (2004).

[30] N. Olanj, M. Lotfi Parsa, and L. Asgari, Analytical solution of the DGLAP equations using the generating function method, Phys. Lett. B **834,** 137472 (2022).

[31] B. Guiot and A. van Hameren, Examination of k_t-factorization in a Yukawa theory, J. High Energy Phys. 04 (2024) 085.

[32] H. Hosseinkhani, M. Modarres, and N. Olanj, Transverse momentum dependent (TMD) parton distribution functions generated in the modified DGLAP formalism based on the valence-like distributions, Int. J. Mod. Phys. A **32,** 1750121 (2017).

[33] M. Modarres, M. R. Masouminia, H. Hosseinkhani, and N. Olanj, The proton FL dipole approximation in the KMR and the MRW unintegrated parton distribution functions frameworks, Nucl. Phys. **A945,** 168 (2016).

[34] M. Modarres, H. Hosseinkhani, N. Olanj, and M. R. Masouminia, A new phenomenological investigation of KMR and MRW unintegrated parton distribution functions, Eur. Phys. J. C **75,** 556 (2015).

[35] M. Modarres, H. Hosseinkhani, and N. Olanj, Phenomenological study of unintegrated parton distribution functions in the frameworks of the Kimber-Martin-Ryskin and Martin-Ryskin-Watt approaches, Phys. Rev. D **89,** 034015 (2014).

[36] M. Modarres, H. Hosseinkhani, and N. Olanj, The NLO unintegrated parton distribution functions (PDF) in the KMR and the MRW frameworks using the MSTW2008 PDF, Nucl. Phys. **A902,** 21 (2013).

[37] M. Modarres and H. Hosseinkhani, The Kimber–Martin–Ryskin unintegrated partons via the MRST and GRV parametrizations, Nucl. Phys. **A815,** 40 (2009).

[38] H. Hosseinkhani and M. Modarres, The general behavior of NLO unintegrated parton distributions based on the single-scale evolution and the angular ordering constraint, Phys. Lett. B **694,** 355 (2011).

[39] H. Hosseinkhani and M. Modarres, The LO and the NLO unintegrated parton distributions in the modified DGLAP formalism, Phys. Lett. B **708,** 75 (2012).

[40] M. Modarres, M. R. Masouminia, R. Aminzadeh-Nik, H. Hoseinkhani, and N. Olanj, NLO production of $W^{\pm}$ and Z^0 vector bosons via hadron collisions in the frameworks of Kimber-Martin-Ryskin and Martin-Ryskin-Watt unintegrated parton distribution functions, Phys. Rev. D **94,** 074035 (2016).

[41] M. Modarres, M. R. Masouminia, R. Aminzadeh-Nik, H. Hoseinkhani, and N. Olanj, KMR k_t-factorization procedure for the description of the LHCb forward hadron–hadron Z^0 production at $\sqrt{s} = 13$ TeV, Phys. Lett. B **772,** 534 (2017).

[42] M. Modarres, M. R. Masouminia, R. Aminzadeh-Nik, H. Hoseinkhani, and N. Olanj, Semi-NLO production of Higgs bosons in the framework of k_t-factorization using KMR unintegrated parton distributions, Nucl. Phys. **B926,** 406 (2018).

[43] M. Modarres, M. R. Masouminia, R. Aminzadeh-Nik, H. Hoseinkhani, and N. Olanj, LHC production of forward-center and forward-forward di-jets in the k_t-factorization and transverse dependent unintegrated parton distribution frameworks, Nucl. Phys. **B922,** 94 (2017).

[44] M. Modarres, R. Aminzadeh-Nik, R. Kord Valeshbadi, H. Hosseinkhani, and N. Olanj, LHC production of forward-center and forward-forward di-jets in the k_t-factorization and transverse dependent unintegrated parton distribution frameworks, Nucl. Phys. B **922,** 94 (2017).

[45] R. Aminzadeh Nik, M. Modarres, N. Olanj, and R. Taghavi, $p - p(\bar{p})$ cross section of isolated single photon production in the k_t-factorization and different angular ordering unintegrated parton distributions frameworks, Phys. Rev. D **103,** 074020 (2021).

[46] R. K. Valeshabadi, M. Modarres, S. Rezaie, and R. Aminzadeh-Nik, Inclusive jet and dijet productions using k_t and (z, k_t)-factorizations versus ZEUS collaboration data,, J. Phys. G **48,** 085009 (2021).

[47] R. K. Valeshabadi, M. Modarres, and S. Rezaie, Validity check of the KATIE parton level event generator in the k_t-factorization and collinear frameworks, Phys. Rev. D **104**, 054019 (2021).

[48] R. K. Valeshabadi, M. Modarres, and S. Rezaie, Three-photon productions within the k_t-factorization at the LHC, Eur. Phys. J. C **81**, 961 (2021).

[49] S. Rezaie and M. Modarres, Investigation of the Z boson production via hadron–hadron collisions in the k_t and (z, k_t)-factorization frameworks, Eur. Phys. J. C **83**, 678 (2023).

[50] W. Furmanski and R. Petronzio, Singlet parton densities beyond leading order, Phys. Lett. **97B**, 437 (1980).